



Phylogenetic relationships of *Chacodelphys* (Marsupialia: Didelphidae: Didelphinae) based on “ancient” DNA sequences

JUAN F. DÍAZ-NIETO,* SHARON A. JANSA, AND ROBERT S. VOSS

Department of Ecology, Evolution, and Behavior and J. F. Bell Museum of Natural History, University of Minnesota, 1987 Upper Buford Circle, St. Paul, MN 55108, USA (JFD, SAJ)

Division of Vertebrate Zoology (Mammalogy), American Museum of Natural History, Central Park West at 79th Street, New York, NY 10024, USA (RSV)

* Correspondent: diaz0154@umn.edu

Morphological character data are inadequate to resolve the evolutionary relationships of the didelphid genus *Chacodelphys*, which previous phylogenetic analyses have alternatively suggested might be the sister taxon of *Lestodelphys* and *Thylamys* (tribe Thylamyini) or of *Monodelphis* (tribe Marmosini) in the subfamily Didelphinae. Because fresh material of *Chacodelphys* is unavailable, we extracted DNA from microscopic fragments of soft tissue adhering to the 95-year-old holotype skull of *C. formosa*. Phylogenetic analyses of the resulting sequence data convincingly resolve *Chacodelphys* as the sister taxon of *Cryptonanus*, a genus with which it had not previously been thought to be closely related. This novel clade (*Chacodelphys* + *Cryptonanus*) belongs to an unnamed thylamyine lineage with *Gracilinanus* and *Lestodelphys* + *Thylamys*, but relationships among these taxa remain to be convincingly resolved.

Los análisis basados en caracteres morfológicos han sido inadecuados para resolver las relaciones evolutivas del género marsupial didélfido *Chacodelphys*. Previos análisis filogenéticos han sugerido como hipótesis alternativas que *Chacodelphys* sea el grupo hermano de *Lestodelphys* y *Thylamys* (tribu Thylamyini) o de *Monodelphis* (tribu Marmosini), todos estos géneros pertenecientes a la subfamilia Didelphinae. Debido a la ausencia de material fresco de *Chacodelphys*, extrajimos ADN de fragmentos microscópicos de tejido adherido al cráneo de 95 años del holotipo de *C. formosa*. Análisis filogenéticos de las secuencias obtenidas resuelven convincentemente la posición filogenética de *Chacodelphys* como el taxón hermano de *Cryptonanus*, un género con el cual nunca antes se había pensado que estuviera cercanamente relacionado. Aunque reconocemos a este nuevo clado (*Chacodelphys* + *Cryptonanus*) junto con *Gracilinanus* y *Lestodelphys* + *Thylamys* pertenecientes a un linaje sin nombre, las relaciones entre estas taxa siguen sin estar convincentemente resueltas.

Key words: *Chacodelphys formosa*, Didelphidae, DNA, phylogeny, Thylamyini

© 2015 American Society of Mammalogists, www.mammalogy.org

The didelphid species *Chacodelphys formosa* has remained a phylogenetic enigma for more than a decade since the genus *Chacodelphys* was proposed by Voss et al. (2004) for “*Marmosa*” *formosa* Shamel, 1930. At that time, *C. formosa* was known from a single specimen collected in the Chaco of northern Argentina in 1920 by the ornithologist Alexander Wetmore. Phylogenetic analyses of morphological character data that Voss et al. (2004) obtained from the holotype skin and skull suggested that *C. formosa* belonged to the subfamily Didelphinae, but different sets of characters tended to place this taxon either with *Lestodelphys* and *Thylamys* (tribe Thylamyini) or with *Monodelphis* (tribe Marmosini). Although subsequent analyses of larger datasets suggested that *Chacodelphys* was a

thylamyine rather than a marmosine, this result was not consistently strongly supported, and different analytic permutations placed the genus either as the sister taxon of *Lestodelphys* + *Thylamys* or as an unresolved polytomy with other thylamyine genera (Voss and Jansa 2009). As discussed by Voss et al. (2004), this phylogenetic uncertainty resulted from conflicting patterns of morphological homoplasy and from the absence of relevant molecular sequence data.

Chacodelphys formosa was rediscovered by Argentinean mammalogists in 2006, but the phylogenetic situation was unimproved because none of the new material was suitable for DNA sequencing. Most of the recently collected specimens are partial skulls recovered from owl pellets, and one

is a skull extracted from a formalin-preserved head (Teta et al. 2006; Teta and Pardiñas 2007). Therefore, the 95-year-old holotype currently remains the only potential source of molecular data.

Here, we report the results of phylogenetic analyses of mitochondrial and nuclear sequences that we obtained by nondestructive sampling of dried soft tissue from the almost completely cleaned holotype skull of *Chacodelphys formosa*. Although sparse, these data are sufficient to identify the sister taxon of *Chacodelphys* with high confidence, and they underscore the potential usefulness of old osteological material for molecular systematics when other sources of crucial sequence data are unavailable. Additionally, our results provide a more densely taxon-sampled thylamyine phylogeny than any previously available in the literature, and they raise interesting questions about morphological trait evolution in this still poorly understood didelphid tribe.

MATERIALS AND METHODS

Source of “ancient” DNA.—We were not allowed to remove integumental fragments from the holotype skin of *Chacodelphys formosa*, a specimen in the National Museum of Natural History (USNM 236330), but permission was given to place the holotype skull in distilled water for several minutes and then to use jewelers’ forceps to remove small amounts of rehydrated soft tissue adhering to cranial bones. Although the skull (Fig. 1) appeared to be completely clean, microscopic examination revealed loose periosteum (membranous connective tissue) covering many surfaces as well as small fragments of muscle in various places and relatively abundant alveolar epithelium surrounding the teeth. This material was carefully harvested, preserved in 95% ethanol, and subsequently stored at -20°C prior to DNA extraction.

Sources of other material.—All other voucher specimens and associated tissues sampled for this study are preserved in the following collections: AMNH, American Museum of Natural History (New York); CBF, Colección Boliviana de Fauna (La Paz); CM, Carnegie Museum of Natural History (Pittsburg); CNP, Centro Nacional Patagónico (Puerto Madryn); CTUA, Colección Teriológica Universidad de Antioquia (Medellín); EBRG, Museo de la Estación Biológica de Rancho Grande (Maracay); FMNH, Field Museum of Natural History (Chicago); MSB, Museum of Southwestern Biology, University of New Mexico (Albuquerque); MUSM, Museo de Historia Natural, Universidad Nacional Mayor de San Marcos (Lima); MVZ, Museum of Vertebrate Zoology, University of California (Berkeley); MZUSP, Museu de Zoologia Universidade de São Paulo (São Paulo); OMNH, Sam Noble Oklahoma Museum of Natural History, University of Oklahoma, (Norman); ROM, Royal Ontario Museum (Toronto); UMMZ, University of Michigan, Museum of Zoology (Ann Arbor); UMSNH, Universidad Michoacana de San Nicolas de Hidalgo (Morelia); USNM, United States National Museum of Natural History (Washington); UWZ, University of Wisconsin Zoological Museum (Madison).



Fig. 1.—Dorsal and ventral views of the holotype skull of *Chacodelphys formosa* (USNM 236330) before tissue harvesting. Note the almost complete absence of macroscopic dried soft tissue.

Taxon and gene sampling.—The designated ingroup for our analyses included 57 representatives of the didelphid subfamily Didelphinae (Table 1). Within Didelphinae, our sampling for the tribes Didelphini, Marmosini, and Metachirini was the same as in Voss et al. (2004), but we follow subsequent taxonomic revisions in using *Monodelphis peruviana* for the material that Voss et al. (2004) called *M. adusta* (see Solari 2007), in using *M. scalops* for the species they called *M. theresa* (see Pavan et al. 2014), and in using *Marmosa* in binomial combinations with the epithets they referred to *Micoureus* (Voss and Jansa 2009). Our sampling for the tribe Thylamyini is the most complete yet achieved in any published phylogenetic analysis; notably, it includes nearly all of the currently recognized valid species of *Cryptonanus*, *Gracilinanus*, *Marmosops*, and *Thylamys*. However, samples of *Cryptonanus agricolai* were unavailable for this study, and we omit *C. ignitus* and *Gracilinanus dryas* because we were unable to resolve these nominal taxa as lineages distinct from *C. chacoensis* and *G. marica*, respectively, based on cytochrome *b* (*Cytb*) sequence data. Our use of *Marmosops fuscatus* (for *M. cracens*), our use of *M. cauae* (for *M. neblina*), and our omission of *M. impavidus* are explained by Díaz-Nieto et al. (in press). We used 2 species of *Caluromys* (subfamily Caluromyinae) as outgroups.

We compiled a multi-locus matrix with sequence data from 1 mitochondrial gene (*Cytb*) and 5 nuclear markers: a fragment of exon 11 from the Breast Cancer type 1 susceptibility gene (*BRCA1*), exon 1 from the gene encoding the Interphotoreceptor

Table 1.—List of taxa and loci included in our analyses. Unshaded cells represent sequences obtained from Genbank (see text), and highlighted cells are new sequences obtained for this work.

Species	Voucher	<i>Cytb</i>	<i>BRCA1</i>	<i>IRBP</i>	<i>Anon128</i>	<i>OGT</i>	<i>SLC38</i>
<i>Caluromys derbianus</i>	USNM 578119	1,140	948	1,158	636	662	730
<i>Caluromys lanatus</i>	ROM 104570	1,140	948	1,158	636	666	730
<i>Chacodelphys formosa</i>	USNM 236330	237	376				
<i>Chironectes minimus</i>	ROM 98855	1,140	942	1,158	638	591	620
<i>Cryptonanus chacoensis</i>	GD521 (to be catalogued at MNHP)	1,140	951	810	635	636	762
<i>Cryptonanus guahybae</i>	FQ23 (to be catalogued at FURB)	313			637	636	681
<i>Cryptonanus unduaviensis</i>	AMNH 260032	715	951	1,158	637	632	530
<i>Didelphis albiventris</i>	UMMZ 134058	1,140	942	1,158	645	651	786
<i>Didelphis marsupialis</i>	chimera (see Supporting Information S2)	1,140	942	1,158	646	651	540
<i>Didelphis virginiana</i>	ROM 96483	1,140	942	1,158	647	651	540
<i>Gracilinanus aceramarcae</i>	MUSM 13002	1,133	951	1,158	637	621	602
<i>Gracilinanus agilis</i>	MVZ 197439	1,140	951	1,158	557	625	745
<i>Gracilinanus emiliae</i>	MUSM 15292	1,140	951	1,158	636	626	356
<i>Gracilinanus marica</i>	EBRG 24864	1,140	618	1,158	533	626	628
<i>Gracilinanus microtarsus</i>	MVZ 182056	1,140	951	1,155	508	621	822
<i>Gracilinanus peruanus</i>	LHE1676a (to be catalogued at MNK)	692	909	547	635	626	750
<i>Lestodelphys halli</i>	chimera (see Supporting Information S2)	1,140	353	1,158	614	644	602
<i>Lutreolina crassicaudata</i>	UMMZ 134019	1,140	942	1,154	643	651	547
<i>Marmosa demerarae</i>	ROM 113431	1,140	948	1,158	637	645	
<i>Marmosa lepida</i>	chimera (see Supporting Information S2)	1,140	948	1,158	637	645	639
<i>Marmosa mexicana</i>	chimera (see Supporting Information S2)	1,140	881	1,158	625	657	613
<i>Marmosa murina</i>	chimera (see Supporting Information S2)	1,140	929	1,158	617	644	642
<i>Marmosa paraguayana</i>	MVZ 182065	1,140	948	1,158	637	645	632
<i>Marmosa regina</i>	MVZ 190332	1,140	942	1,158	594	637	709
<i>Marmosa robinsoni</i>	AMNH 276746	1,132	884	1,146	637	664	629
<i>Marmosa rubra</i>	chimera (see Supporting Information S2)	1,140	948	1,158	630	362	345
<i>Marmosops bishopi</i>	FMNH 203328	1,140	880	1,158	648	653	769
<i>Marmosops caucae</i>	MVZ 190272	1,140	886	1,158	600	667	521
<i>Marmosops creightoni</i>	CBF 7641	1,140	886	1,158	645	673	771
<i>Marmosops fuscatus</i>	AMNH 276509	1,140	889	1,149	582	657	782
<i>Marmosops handleyi</i>	CTUA 415	1,140	883	1,149	591	658	786
<i>Marmosops incanus</i>	chimera (see Supporting Information S2)	1,140	883	1,158	638	631	674
<i>Marmosops invictus</i>	USNM 337962	483	388				
<i>Marmosops juminensis</i>	AMNH 230016		930		553	639	604
<i>Marmosops noctivagus</i>	MUSM 13292	1,140	882	1,158	527	670	
<i>Marmosops ocellatus</i>	USNM 581979	1,140	886	1,158	554	669	745
<i>Marmosops ojasii</i>	USNM 371299	391	882			503	
<i>Marmosops pakaraimae</i>	ROM 115841	645	886	1,158	581	573	775
<i>Marmosops parvidens</i>	ROM 97938	645	945	1,158	580	545	678
<i>Marmosops paulensis</i>	MVZ 183244	1,140	886	1,158	577	634	705
<i>Marmosops pinheiroi</i>	chimera (see Supporting Information S2)	1,140	945	1,158	641	574	763
<i>Metachirus nudicaudatus</i>	ROM 105345	1,140	942	1,158	641	523	759
<i>Monodelphis breviceaudata</i>	ROM 98909	1,140	945	1,158	637	650	876
<i>Monodelphis emiliae</i>	MUSM 13298	795	945	1,158	634	650	865
<i>Monodelphis peruviana</i>	AMNH 272695	795	945	1,158	636	649	854
<i>Monodelphis scalops</i>	MVZ 182776	1,140	945	1,158	626	644	875
<i>Philander frenatus</i>	MVZ 182067	1,140	942	1,158	538	641	783
<i>Philander mcilhennyi</i>	AMNH 272818	1,140	942	1,158	590	642	783
<i>Philander opossum</i>	CM 76743	1,140	942	732	565	641	757
<i>Thylamys elegans</i>	MSB 87097	1,140	951	1,158	646	654	513
<i>Thylamys karimii</i>	MZUSP 32094	1,140	954	548	581	653	470
<i>Thylamys macrurus</i>	MSB 70700	1,140	951	1,158	648	653	513
<i>Thylamys pallidior</i>	chimera (see Supporting Information S2)	1,140	951	1,134	643	645	513
<i>Thylamys pusillus</i>	MSB 67016	1,140	951	1,158	648	653	516
<i>Thylamys sponsorius</i>	FMNH 162505	1,140	930	1,158	648	653	756
<i>Thylamys tatei</i>	MVZ 135504	1,140					
<i>Thylamys velutinus</i>	OMNH 37216	1,140					
<i>Thylamys venustus</i>	AMNH 275428	1,140	951	1,102	648	653	513
<i>Tlacuatzin canescens</i>	UMSNH 2993	1,140	948	1,158	630	618	731

Retinoid-Binding Protein (*IRBP*), intron 14 of the X chromosome-linked O-linked *N*-acetylglucosamine transferase (*OGT*), intron 7 from the autosomal gene sodium-coupled neutral

amino acid transporter 2 (*SLC38*), and an anonymous locus (*Anon128*, corresponding to a marker originally recovered for the genus *Thylamys*—Giarla et al. 2014). Some of these

data (the unshaded cells in Table 1) were downloaded from Genbank, where they had previously been archived following earlier studies by our lab (Jansa and Voss 2000; Voss and Jansa 2003, 2009; Voss et al. 2005, 2013, 2014; Giarla et al. 2010, 2014; Gutiérrez et al. 2010; Giarla and Jansa 2014), but we also generated many new sequences for this work (the shaded cells in Table 1).

Laboratory methods and sequence alignment.—We extracted DNA either from preserved tissue or from dried museum specimens following procedures explained in Voss and Jansa (2009) and Giarla et al. (2010), respectively. All the markers implemented in this study were amplified using polymerase chain reaction (PCR) methods. To minimize the risk of contamination, ancient DNA extraction and corresponding PCR amplifications were carried out in a laboratory where mammalian DNA amplified from fresh tissue has never been present. Primers for the loci *Cytb*, *BRCA1*, *IRBP*, *OGT*, and *SLC38* were described in Jansa and Voss (2000); Giarla et al. (2010); Voss et al. (2014); and Díaz-Nieto et al. (in press). The anonymous locus (*Anon128*) was obtained using primers modified from those in Giarla et al. (2014), and for thylamyine species we designed new primers for *SLC38*. Additionally, due to the highly degraded “ancient” DNA obtained from *Chacodelphys*, we obtained a small fragment each of *Cytb* and *BRCA1* (in a single reaction for each gene) using internal primers. All the new primers designed for this study, including those used to amplify *Chacodelphys* sequences, can be found in Supporting Information S1. Amplification protocols for *Cytb*, *BRCA1*, *IRBP*, *OGT*, and *SLC38* closely resembled those described in Voss et al. (2014), and amplification protocols for *Anon128* can be found in Giarla et al. (2014). The resulting PCR products were sequenced using amplification primers and dye-terminator chemistry on an ABI-3730x1 automated sequencer. For the nuclear genes, heterozygous indels were detected and phased using the software Indelligent v.1.2 (Dmitriev and Rakitov 2008). Sequences were assembled using Sequencher ver. 4.8 (Gene Codes Corporation, Ann Arbor, Michigan) and aligned using the default settings of MUSCLE (Edgar 2004) in Geneious Pro ver. 5.6.3 created by Biomatters (available from <http://www.geneious.com>). The resulting alignments (of protein-coding genes) were inspected with reference to translated amino acid sequences. All new sequences obtained for this study have been deposited in GenBank: *Anon128* (KU171130–KU171171), *BRCA1* (KU171172–KU171184), *Cytb* (KU171185–KU171199), *IRBP* (KU171200–KU171219), *OGT* (KU171220–KU171245), and *SLC38* (KU171246–KU171275).

Phylogenetic analyses.—We generated gene trees from independent phylogenetic analyses of each of the 6 loci sampled for this study, and we also performed phylogenetic analyses on concatenated gene datasets. For the latter analyses, we evaluated 2 different concatenations: one with just the 2 loci from which sequence data were obtained for *Chacodelphys* (*Cytb* + *BRCA1*) and a second including all of the mitochondrial and nuclear markers (*Cytb* + nucDNA). Unless noted otherwise, all phylogenetic analyses were implemented through the CIPRES Science Gateway (Miller et al. 2010). Each of the protein-coding genes (*Cytb*, *BRCA1*, and *IRBP*) was partitioned by codon

position, and the Bayesian Information Criterion (BIC) implemented in PartitionFinder (Lanfear et al. 2012) was used to determine the best partitioning scheme and substitution models (Table 2). The nuclear introns and the anonymous locus were each analyzed as a single partition, and the best-fitting nucleotide substitution model was determined under the BIC in jModelTest 2 (Darriba et al. 2012). Gene trees were subsequently generated using Bayesian Inference (BI) and Maximum Likelihood (ML) searches. In all instances, Bayesian Inference was implemented in MrBayes v3.2 (Ronquist et al. 2012) by running 2 independent Markov Chain Monte Carlo (MCMC) analyses including 1 cold chain and 3 heated chains. For the non-coding genes, the length of the chain was 2×10^6 generations, sampling every 200 generations and implementing the optimal substitution model from jModelTest. Because initial runs for the protein-coding genes did not converge after 2×10^6 generations, we increased the length of the chain to 4×10^6 generations, sampling every 400 generations and implementing the optimal partitioning scheme and substitution model from PartitionFinder. We evaluated convergence and appropriate burnin values by examining the results of the MCMC runs in Tracer v1.5 (Rambaut and Drummond 2007). For each of the BI analyses, all parameters were summarized in a maximum clade credibility tree with TreeAnnotator v1.7.2 (Drummond et al. 2012). Maximum likelihood analyses for each locus were implemented in RAxML ver. 8.0 (Stamatakis 2014). For the coding genes, we implemented the optimal partition scheme from PartitionFinder and the GTRGAMMA as substitution model; each of the non-coding genes was analyzed as a single partition with the GTRGAMMA model. We implemented 20 independent searches from which we chose the topology with the best lnL score. Subsequently, we evaluated nodal support by running 1,000 bootstrap replicates using the GTRGAMMA model and the “thorough” optimization option. Bipartitions of the bootstrap searches were summarized on the best ML topology.

For the 2 concatenated gene datasets, we determined the optimal partitioning scheme and substitution models using the *greedy* search algorithm and BIC implemented in PartitionFinder (Lanfear et al. 2012). For the 2 datasets, we partitioned the protein-coding genes by locus and by codon position, and we used a single partition for each of the non-coding nuclear genes: 6 partitions were analyzed for the *Cytb* + *BRCA1* dataset and 12 partitions for the *Cytb* + nucDNA dataset. Optimal partitioning schemes and substitution models can be found in Table 2. Multi-locus partitioned datasets were analyzed using Bayesian Inference (BI) and Maximum Likelihood (ML) searches implementing the best partition scheme from PartitionFinder and following the same strategies as described for the gene trees with a few exceptions. Bayesian analyses of the *Cytb* + *BRCA1* dataset were run for 2×10^7 generations, sampling every 2,000 generations, whereas the length of the chain for the *Cytb* + nucDNA dataset was 4×10^7 generations, sampling every 4,000 generations.

Hypotheses testing.—Previous phylogenetic analyses have recovered *Chacodelphys* in 2 alternative positions within the

subfamily Didelphinae: as the sister taxon of *Lestodelphys* + *Thylamys* in the tribe Thylamyini (Voss et al. 2004: figure 3; Voss and Jansa 2009: figure 27) or as the sister taxon of *Monodelphis* in the tribe Marmosini (Voss et al. 2004: figure 4). To test these alternative hypotheses against our results, we used Shimodaira–Hasegawa (SH) tests (Shimodaira and Hasegawa 1999) and the approximately unbiased (AU) test of Shimodaira (2002). Although both SH and AU tests are excellent in controlling for type 1 errors, the SH test is thought to be too conservative in some circumstances, and this bias is corrected for by the AU test (Shimodaira 2002). We performed ML analyses in RAxML as described above for 4 different alignments (*Cytb*, *BRCA1*, *Cytb* + *BRCA1*, *Cytb* + nucDNA) with the only difference that we used topological constraints to infer the best tree that conformed to the alternative hypotheses (Table 3). We implemented SH and AU tests in CONSEL v0.20 (Shimodaira and Hasegawa

2001); however, because CONSEL does not estimate the likelihoods for the topologies itself, we first obtained the site likelihoods of each alignment in TREE-PUZZLE 5.3 (Schmidt et al. 2002). Subsequently using CONSEL, the SH test was implemented allowing 1,000 resampling estimated log likelihoods (RELL) replicates, and for the AU test 10,000 multiscale bootstraps were performed also using the RELL method.

RESULTS

Taxon/gene coverage and sequence description.—Our multi-locus dataset contains 179 newly generated sequences, 175 sequences downloaded from Genbank, and 26 missing sequences for a total of 92.7% sequence coverage (Table 1). We obtained *Cytb* sequences for all taxa except *M. juninensis*, a species for which we consistently co-amplified a nuclear pseudogene from our only available sample (a scrap of dried skin). Only 2 species (*Thylamys tatei* and *T. velutinus*) completely lack nuclear sequence data (because the DNA we obtained from dried skins of these taxa was highly degraded). Although we tested several combinations of primers for *C. formosa* to amplify as much sequence as possible from as many loci as possible, we could only successfully amplify and sequence short fragments of *Cytb* and *BRCA1* from this taxon. Finally, for 9 species (identified as chimeras in column 2 of Table 1), it was necessary to combine sequences from different voucher specimens to maximize gene coverage (Supporting Information S2).

Our concatenated gene alignments contained 2,097 base pairs (bp) for *Cytb* + *BRCA1*, and 5,893 bp for *Cytb* + nucDNA (*Cytb*: 1,140 bp; *BRCA1*: 957 bp; *IRBP*: 1,158 bp; *OGT*: 840 bp; *SLC38*: 1,124 bp; *Anon128*: 674 bp). Base compositional heterogeneity tests were not significant for the individual gene alignments *BRCA1*, *IRBP*, *OGT*, *SLC38*, and *Anon128*, but significant heterogeneity was found for *Cytb* and for our 2 concatenated datasets (Table 4). However, critical values of the “gI” skewness test statistic (Hillis and Huelsenbeck 1992) suggest that the observed base frequencies are non-random and that there is significant ($P < 0.01$) phylogenetic signal in all of our single gene and concatenated alignments.

Phylogenetic results.—Gene trees that we obtained from phylogenetic analyses of *Cytb* (Fig. 2) and *BRCA1* (Fig. 3) both recovered *Chacodelphys* as a member of the tribe Thylamyini,

Table 2.—Optimal partitioning schemes and substitution models for *Cytb*, *BRCA1*, *IRBP*, and 2 concatenated gene datasets.

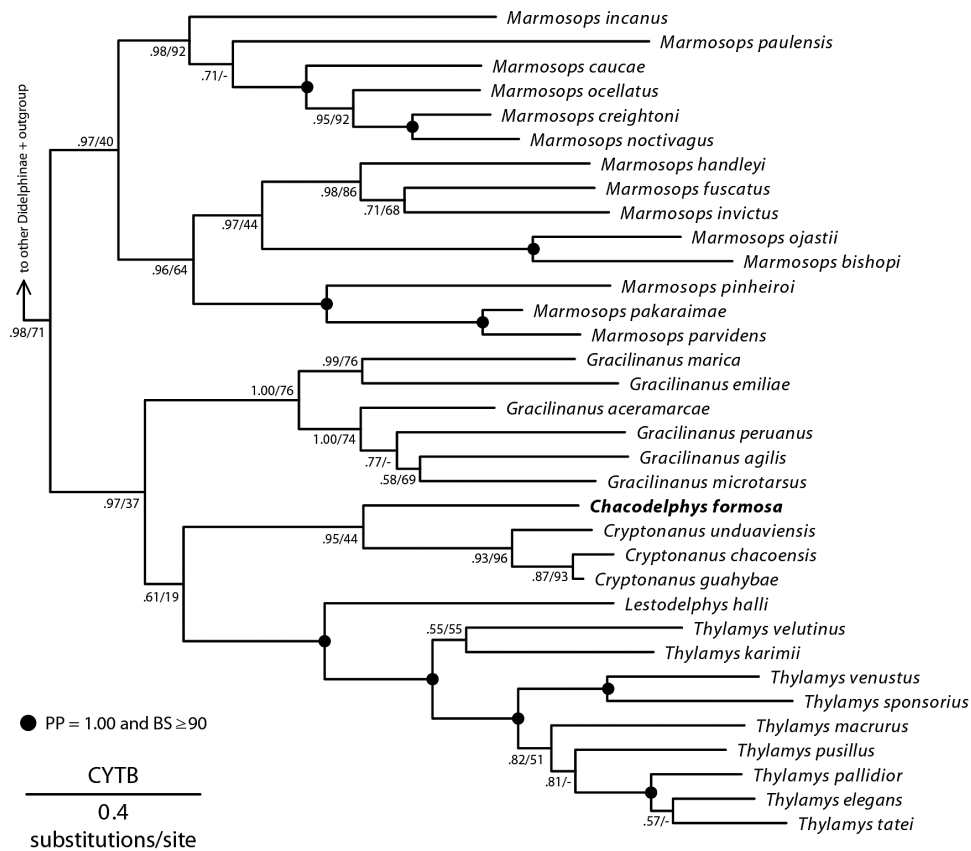
Name	Partition #	Characters	Model
<i>Cytb</i>	1	<i>Cytb</i> position 1	GTR+I+Γ
	2	<i>Cytb</i> position 2	HKY+I+Γ
	3	<i>Cytb</i> position 3	HKY+I+Γ
<i>BRCA1</i>	1	<i>BRCA1</i> positions 1 and 2	HKY+Γ
	2	<i>BRCA1</i> position 3	HKY+Γ
<i>IRBP</i>	1	<i>IRBP</i> position 1	HKY+I+Γ
	2	<i>IRBP</i> position 2	HKY+I
	3	<i>IRBP</i> position 3	K80+Γ
<i>Cytb</i> + <i>BRCA1</i>	1	<i>BRCA1</i> positions 1 and 2	HKY+Γ
	2	<i>BRCA1</i> position 3	HKY+Γ
	3	<i>Cytb</i> position 1	GTR+I+Γ
<i>Cytb</i> + nucDNA	4	<i>Cytb</i> position 2	HKY+I+Γ
	5	<i>Cytb</i> position 3	HKY+I+Γ
	1	<i>BRCA1</i> positions 1 and 2	HKY+Γ
	2	<i>BRCA1</i> position 3	HKY+Γ
	3	<i>Cytb</i> position 1	GTR+I+Γ
	4	<i>Cytb</i> position 1, <i>IRBP</i> position 1	HKY+I+Γ
	5	<i>Cytb</i> position 3	GTR+I+Γ
	6	<i>IRBP</i> position 1	HKY+I
	7	<i>IRBP</i> position 3, <i>OGT</i>	K80+Γ
8	<i>Anon128</i>	K80+Γ	
9	<i>SLC38</i>	SYM+Γ	

Table 3.—Shimodaira–Hasegawa (SH) and approximately unbiased (AU) topology tests for 4 different alignments. We tested the phylogenetic position of *Chacodelphys formosa* obtained in the present work (hypothesis 1) against 2 alternative hypotheses. Significance levels indicating statistical rejection of hypotheses 2 or 3 are denoted by asterisks: < 0.05 (*), < 0.01 (**), and < 0.001 (***).

Alternative hypotheses	<i>Cytb</i>		<i>BRCA1</i>		<i>Cytb</i> + <i>BRCA1</i>		<i>Cytb</i> + nucDNA	
	AU	SH	AU	SH	AU	SH	AU	SH
1. <i>Chacodelphys</i> + <i>Cryptonanus</i>	0.766	0.901	0.978	0.973	0.991	0.984	0.992	0.987
2. <i>Chacodelphys</i> + <i>Monodelphis</i>	0.044*	0.171	0.000***	0.000***	0.000***	0.000***	0.000***	0.000***
3. <i>Chacodelphys</i> + (<i>Lestodelphys</i> + <i>Thylamys</i>)	0.328	0.408	0.022*	0.235	0.010**	0.202	0.008**	0.149

Table 4.—Chi-square tests for base compositional stationarity and g_1 skewness test statistic (Hillis and Huelsenbeck, 1992).

Alignment	Chi-square test			Skewness test g_1 ($P < 0.01$)		
	χ^2	<i>d.f.</i>	<i>P</i> -value	<i>N</i> variable characters	<i>N</i> taxa	g_1
<i>Cytb</i>	230.157	171	0.002	557	58	−0.491
<i>BRCA1</i>	14.369	165	1.000	338	56	−0.526
<i>IRBP</i>	21.656	153	1.000	218	52	−0.599
<i>OGT</i>	52.726	162	1.000	406	55	−0.593
<i>SLC38</i>	170.963	153	0.152	540	53	−0.473
<i>Anon128</i>	17.216	159	1.000	211	54	−0.891
<i>Cytb</i> + <i>BRCA1</i>	314.163	174	0.000	895	59	−0.510
<i>Cytb</i> + nucDNA	350.095	174	0.000	2,333	59	−0.573

**Fig. 2.**—Bayesian Inference topology detailing the phylogenetic relationships of *Chacodelphys formosa* within the tribe Thylamyini using *Cytb* sequences. Posterior probabilities (PPs) below 1.00 and bootstrap support (BS) values below 90% are shown along branches (PP/BS), whereas PP of 1.00 and BS $\geq 90\%$ are indicated with filled circles at relevant nodes. Outgroup and other non-thylamyine species are not shown.

to which we restrict our attention hereafter. Within Thylamyini, *Chacodelphys* was consistently recovered in a clade that also included *Cryptonanus*, *Gracilinanus*, *Lestodelphys*, and *Thylamys*. Within the latter group, both genes also recovered *Chacodelphys* as the sister taxon of *Cryptonanus*, a previously unsuspected relationship that is strongly supported by *BRCA1* and less so by *Cytb*. This new clade (*Chacodelphys* + *Cryptonanus*) was recovered as the sister taxon of *Lestodelphys* + *Thylamys* in our analyses of *Cytb* sequences, whereas analyses of *BRCA1* recovered *Chacodelphys* + *Cryptonanus* as the sister taxon of a group that also included *Gracilinanus*. Although the 2 gene trees differ in this and other respects, it is noteworthy that no strongly supported node in one topology is incompatible with any strongly supported node in the other, so it seems

reasonable to analyze the concatenated sequences obtained from these largely congruent loci. Analyses of this 2-gene dataset (Fig. 4) resulted in strong support for many thylamyine nodes that were only weakly supported in the individual gene trees, and they recovered *Chacodelphys* + *Cryptonanus* as the sister taxon of *Lestodelphys* + *Thylamys* (as in the *Cytb* tree), but without strong support.

Despite the fact that we were unable to amplify and sequence *Chacodelphys* for the other 4 loci we sampled (*IRBP*, *OGT*, *SLC38*, *Anon128*), it seemed plausible that those genes might help resolve its relationships by constraining the position of *Cryptonanus* (for which we have much more extensive sequence data). Inspection of individual gene trees for those loci (Supporting Information S3) revealed no strong

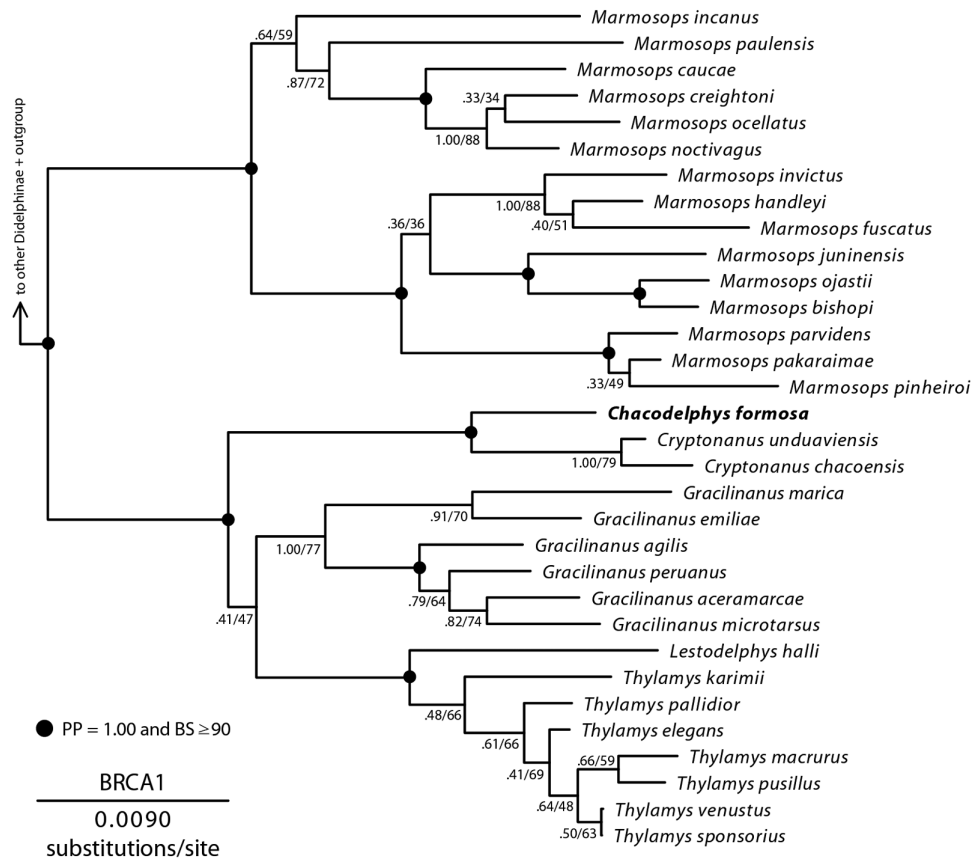


Fig. 3.—Bayesian Inference topology detailing the phylogenetic relationships of *Chacodelphys formosa* within the tribe Thylamyini using *BRCA1* sequences. Posterior probabilities (PPs) below 1.00 and bootstrap support (BS) values below 90% are shown along branches (PP/BS), whereas PP of 1.00 and BS $\geq 90\%$ are indicated with filled circles at relevant nodes. Outgroup and other non-thylamyine species are not shown.

incongruence among them nor is there any strong incongruence between this set of trees and the results we obtained from separate and concatenated analyses of *Cytb* and *BRCA1*. The results of analyzing a matrix of concatenated sequence data from all 6 loci (*Cytb* + nucDNA; Fig. 5) are not essentially different from those we obtained from the concatenated 2-gene analyses insofar as the relationships of *Chacodelphys* are concerned, but several thylamyine nodes that were only weakly supported by *Cytb* + *BRCA1* are strongly supported by this much larger dataset. Unfortunately, the sister group relationship between *Chacodelphys* + *Cryptonanus* and *Lestodelphys* + *Thylamys* remains present but weakly supported.

The topology tests that we performed (Table 4) almost uniformly reject the hypothesis that *Chacodelphys* is the sister taxon of *Monodelphis* (the unique exception is the SH test for *Cytb*). The hypothesis that *Chacodelphys* is the sister taxon of *Lestodelphys* + *Thylamys* is rejected for most datasets by the AU test (the unique exception, again, is *Cytb*), but not by the more conservative SH test.

Although the focus of this report concerns *Chacodelphys*, our results include several other noteworthy contributions to didelphid phylogenetics including 1) strong support for most polytypic thylamyine genera, several of which are here represented by more species than in earlier studies, 2) strong support for a basal dichotomy in *Marmosops*, 3) strong support for

numerous relationships among previously unsequenced species of *Marmosops*, 4) strong support for a sister group relationship between *G. marica* (previously unsequenced) and *G. emiliae*; and 5) strong support for the monophyly of the nominotypical subgenus of *Thylamys*.

DISCUSSION

Although sparse, the sequence data we obtained from *Chacodelphys* (613 bp from 2 loci) seem sufficient to confidently reject at least 2 previously published hypotheses. In particular, the suggestion that *Chacodelphys* might be a marmosine closely related to *Monodelphis* (Voss et al. 2004) now seems highly improbable based on nodal statistics computed from our concatenated 6-gene dataset (Fig. 5) and from the results of topology tests (Table 4). Because *Cytb* sequences are saturated (and therefore phylogenetically uninformative) at deeper levels of didelphid phylogeny (Jansa and Voss 2000: figure 12), the non-significant SH test result and the only marginally significant AU test result from this locus by comparison with those obtained from the more slowly evolving nuclear loci are not surprising. In effect, it now seems reasonably certain that *Chacodelphys* belongs in the tribe Thylamyini.

Within the tribe Thylamyini, nodal statistics (Bayesian posterior probabilities and likelihood bootstrap values) strongly

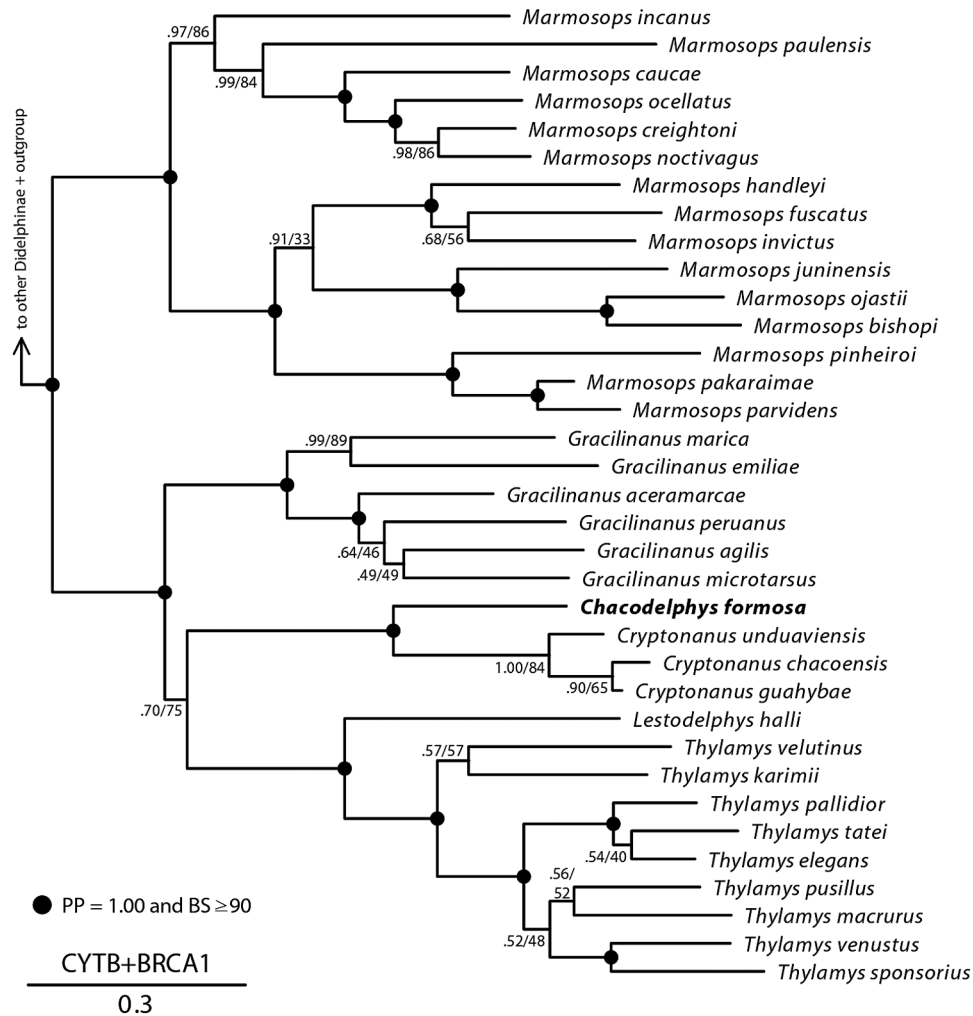


Fig. 4.—Bayesian Inference analysis of the concatenated dataset *Cytb* + *BRCA1* detailing the phylogenetic relationships of *Chacodelphys formosa* within the tribe Thylamyini. Posterior probabilities (PPs) below 1.00 and bootstrap support (BS) values below 90% are shown along branches (PP/BS), whereas PP of 1.00 and BS ≥ 90% are indicated with filled circles at relevant nodes. Outgroup and other non-thylamyine species are not shown.

constrain the plausible relationships of *Chacodelphys* to a rather small set of alternative hypotheses. That *Chacodelphys* appears to be the sister taxon of *Cryptonanus*, although unexpected, is not hard to reconcile with the results of earlier analyses. *Cryptonanus* was not included in the morphology-based phylogenetic study that previously associated *Chacodelphys* with *Lestodelphys* + *Thylamys* or with *Monodelphis* (Voss et al. 2004) because *Cryptonanus* had yet to be recognized as generically distinct from *Gracilinanus* (which was represented in those analyses only by *G. microtarsus*). In subsequent analyses that included *Cryptonanus*, none of the nodes that separated that genus from *Chacodelphys* were strongly supported (Voss and Jansa 2009: figures 27 and 36). Therefore, the sister group relationship reported here is not strongly contradicted by those results.

Nodal statistics likewise exclude *Marmosops* from any close relationship with *Chacodelphys* + *Cryptonanus*, which, instead, belongs to a strongly supported clade with the other 3 thylamyine genera. Thus, what remains for future research to resolve is whether *Chacodelphys* + *Cryptonanus* is more

closely related to *Gracilinanus* (the genus that previously included species that are now placed in *Chacodelphys* and *Cryptonanus*—Voss et al. 2004, 2005) or with *Lestodelphys* + *Thylamys*, another well-supported generic pairing. Extensive missing sequence data from *Chacodelphys* might be part of the reason why these relationships are still in question, but we note that the relationships of *Cryptonanus* with respect to *Gracilinanus* and *Lestodelphys* + *Thylamys* are not convincingly resolved by nuclear sequence datasets that exclude *Chacodelphys* (e.g., in Voss and Jansa 2009), so it is possible that the essential problem is short evolutionary intervals between successive speciation events rather than missing data.

Because *Chacodelphys* and *Cryptonanus* have not previously been recognized as sister taxa, it seems useful to list the phenotypic differences that support their recognition as distinct genera and that suggest that each is adapted to a different ecological niche (Table 5). Judging from its short tail, lack of a caudal prehensile surface, and mesaxonic forefeet, for example, we expect that *Chacodelphys* is almost exclusively

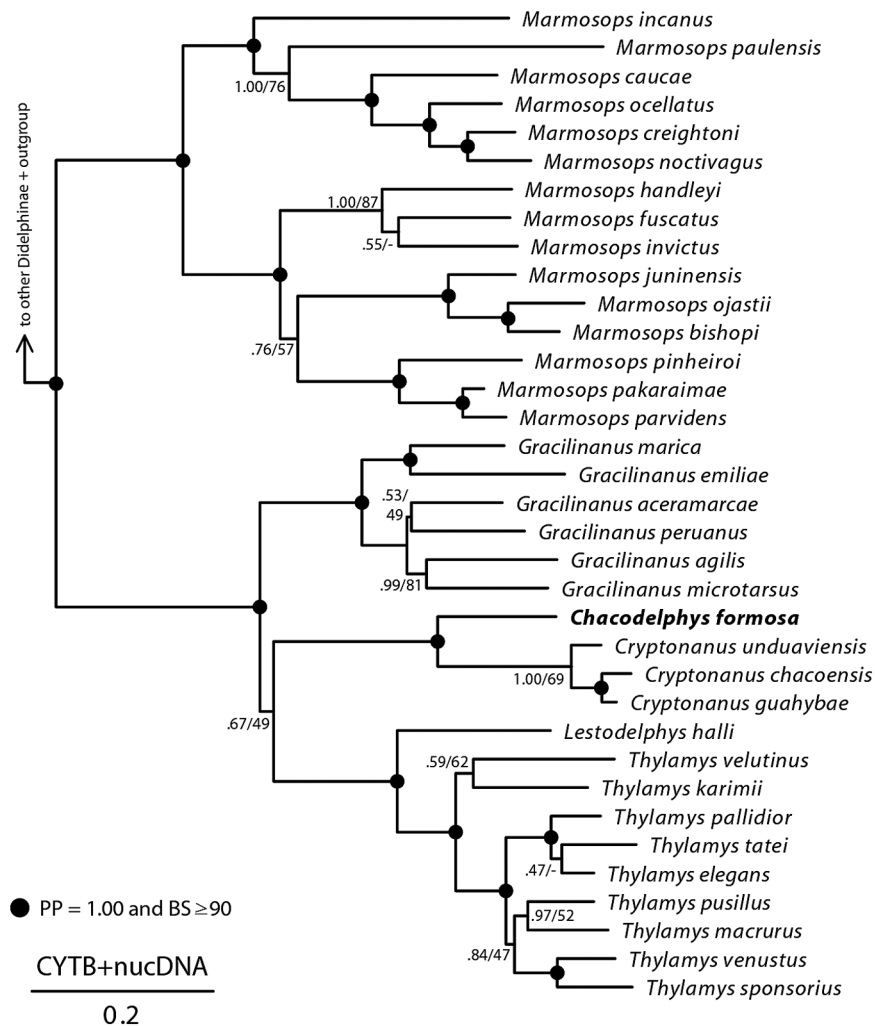


Fig. 5.—Bayesian Inference analysis of the concatenated dataset *Cytb* + nucDNA detailing the phylogenetic relationships of *Chacodelphys formosa* within the tribe Thylamyini. Posterior probabilities (PPs) below 1.00 and bootstrap support (BS) values below 90% are shown along branches (PP/BS), whereas PP of 1.00 and BS ≥ 90% are indicated with filled circles at relevant nodes. Outgroup and other non-thylamyine species are not shown.

Table 5.—Qualitative morphological differences between *Chacodelphys* and *Cryptonanus* (see Voss and Jansa [2009] for explanations of character state descriptors).

Character	<i>Chacodelphys</i>	<i>Cryptonanus</i>
Relative tail length ^a	81%	117–136%
Manus	Mesaxonic ^b	Paraxonic ^c
Central palmar surface of manus	Densely tubercular	Sparsely tubercular
Caudal prehensile surface	Absent	Present
Nasal bones	Uniformly narrow	Widened posteriorly
Maxillary fenestrae	Present	Absent
C1	W/o accessory cusps	Usually w/accessory cusp(s)
P2, P3 heights	P2 = P3	P2 < P3
Hypoconid on m3	Lingual to protoconid	Labially salient
Entoconid, hypoconulid heights	Entoconid ≈ hypoconulid	Entoconid >> hypoconulid

^a Length of tail divided by length of head and body, expressed as a percentage (based on measurement data in Voss et al. 2004, 2005).

^b Digit III longest.

^c Digit III = digit IV.

terrestrial, whereas a contrasting set of traits (longer tail, caudal prehensile surface present, paraxonic forefeet) lead us to expect that *Cryptonanus* is scansorial. Testing for such behavioral differences, which might be correlated with habitat occupancy at localities where these taxa are sympatric (e.g., those mapped by Teta et al. 2006), should be a priority for future field research.

ACKNOWLEDGMENTS

We are thankful to the many curators, collection managers, and collectors who loaned tissues that we used in this project, especially A. Carmignotto (MZUSP); B. Patterson and B. Stanley (FMNH); B. K. Lim (ROM); F. Quintela (for material that will eventually be deposited at FURB); F. Bisbal-E. and J. Sánchez-H. (EBRG); G. D'Elía (for material that will eventually be deposited at MNHP); J. R. Wible and S. B. McLaren (CM); J. L. Patton, E. Lacey, and C. Conroy (MVZ); J. Cook and J. Dunnun (MSB); A. L. Gardner, L. Gordon, and K. M.

Helgen (USNM); L. Emmons (for material that will eventually be deposited at MNK); P. Myers (UMMZ); S. Solari (CTUA); T. Tarifa (CBF); and V. Pacheco (MUSM). We thank C. Martin, L. Fujishin, and T. Giarla for assistance with laboratory work. This work was funded in part by National Science Foundation grants DEB-743039 (to RSV), DEB-743062 (to SAJ), and a Doctoral Dissertation Improvement Grant, Award Number 1311163 (to SAJ and JFD). JFD wants to acknowledge a Grant-in-Aid of Research from the American Society of Mammalogists and the James W. Wilkie Fund for Natural History Fellowship from the J. F. Bell Museum of Natural History (University of Minnesota) for providing additional funding to visit museum collections. JFD is currently supported by a Francisco José de Caldas Fellowship from the Colombian department of science, technology, and innovation (COLCIENCIAS). Critical suggestions by J. Esselstyn and 2 anonymous reviewers helped improve the manuscript.

SUPPORTING INFORMATION

Supporting Information S1.—List of primers used to amplify *Cytb* and *BRCA1* for *Chacodelphys formosa* and primers used to amplify *SLC38* and *Anon128* loci for all taxa.

Supporting Information S2.—Species for which sequences from different specimens were combined as chimeric terminals to improve gene coverage.

Supporting Information S3.—Individual genes trees obtained from MrBayes for loci *IRBP*, *OGT*, *SLC38*, and *Anon128*. Values on branches correspond to Posterior Probabilities.

LITERATURE CITED

- DARRIBA, D., G. L. TABOADA, R. DOALLO, AND D. POSADA. 2012. jModelTest 2: more models, new heuristics and parallel computing. *Nature Methods* 9:772–772.
- DÍAZ-NIETO, J. F., S. A. JANSÁ, R. S. VOSS. In press. DNA sequencing reveals unexpected Recent diversity and an ancient dichotomy in the American marsupial genus *Marmosops* (Didelphidae: Thylamyini). *Zoological Journal of the Linnean Society*. DOI: 10.1111/zoj.12343.
- DMITRIEV, D. A., AND R. A. RAKITOV. 2008. Decoding of superimposed traces produced by direct sequencing of heterozygous indels. *PLoS computational biology* 4:e1000113.
- DRUMMOND, A. J., M. A. SUCHARD, D. XIE, AND A. RAMBAUT. 2012. Bayesian phylogenetics with BEAUti and the BEAST 1.7. *Molecular Biology and Evolution* 29:1969–1973.
- EDGAR, R. C. 2004. MUSCLE: multiple sequence alignment with high accuracy and high throughput. *Nucleic Acids Research* 32:1792–1797.
- GIARLA, T. C., AND S. A. JANSÁ. 2014. The role of physical geography and habitat type in shaping the biogeographical history of a recent radiation of Neotropical marsupials (*Thylamys*: Didelphidae). *Journal of Biogeography* 41:1547–1558.
- GIARLA, T. C., R. S. VOSS, AND S. A. JANSÁ. 2010. Species limits and phylogenetic relationships in the didelphid marsupial genus *Thylamys* based on mitochondrial DNA sequences and morphology. *Bulletin of the American Museum of Natural History* 346:1–67.
- GIARLA, T. C., R. S. VOSS, AND S. A. JANSÁ. 2014. Hidden diversity in the Andes: comparison of species delimitation methods in montane marsupials. *Molecular Phylogenetics and Evolution* 70:137–151.
- GUTIÉRREZ, E. E., S. A. JANSÁ, AND R. S. VOSS. 2010. Molecular systematics of mouse opossums (Didelphidae: *Marmosa*): assessing species limits using mitochondrial DNA sequences, with comments on phylogenetic relationships and biogeography. *American Museum Novitates* 3692:1–22.
- HILLIS, D. M., AND J. P. HUELSENBECK. 1992. Signal, noise, and reliability in molecular phylogenetic analyses. *The Journal of Heredity* 83:189–195.
- JANSÁ, S. A., AND R. S. VOSS. 2000. Phylogenetic studies on didelphid marsupials I. Introduction and preliminary results from nuclear IRBP gene sequences. *Journal of Mammalian Evolution* 7:43–77.
- LANFEAR, R., B. CALCOTT, S. Y. W. HO, AND S. GUINDON. 2012. Partitionfinder: combined selection of partitioning schemes and substitution models for phylogenetic analyses. *Molecular biology and evolution* 29:1695–1701.
- MILLER, M. A., W. PFEIFFER, AND T. SCHWARTZ. 2010. Creating the CIPRES Science Gateway for inference of large phylogenetic trees. *Proceedings of the Gateway Computing Environments Workshop (GCE)* 20:1–8.
- PAVAN, S. E., S. A. JANSÁ, AND R. S. VOSS. 2014. Molecular phylogeny of short-tailed opossums (Didelphidae: *Monodelphis*): taxonomic implications and tests of evolutionary hypotheses. *Molecular Phylogenetics and Evolution* 79:199–214.
- RAMBAUT, A., AND A. J. DRUMMOND. 2007. Tracer v1.5. <http://beast.bio.ed.ac.uk/Tracer>. Accessed 30 July 2015.
- RONQUIST, F., ET AL. 2012. MrBayes 3.2: efficient Bayesian phylogenetic inference and model choice across a large model space. *Systematic Biology* 61:539–542.
- SCHMIDT, H. A., K. STRIMMER, M. VINGRON, AND A. VON HAESLER. 2002. TREE-PUZZLE: maximum-likelihood phylogenetic analysis using quartets and parallel computing. *Bioinformatics* 18:502–504.
- SHIMODAIRA, H. 2002. An approximately unbiased test of phylogenetic tree selection. *Systematic Biology* 51:492–508.
- SHIMODAIRA, H., AND M. HASEGAWA. 1999. Multiple comparisons of log-likelihoods with applications to phylogenetic inference. *Molecular Biology and Evolution* 16:1114–1116.
- SHIMODAIRA, H., AND M. HASEGAWA. 2001. CONSEL: for assessing the confidence of phylogenetic tree selection. *Bioinformatics* 17:1246–1247.
- SOLARI, S. 2007. New species of *Monodelphis* (Didelphimorphia: Didelphidae) from Peru, with notes on *M. adusta* (Thomas, 1897). *Journal of Mammalogy* 88:319–329.
- STAMATAKIS, A. 2014. RAXML version 8: a tool for phylogenetic analysis and post-analysis of large phylogenies. *Bioinformatics* 30:1312–1313.
- TETA, P., AND U. F. J. PARDIÑAS. 2007. Mammalia, Didelphimorphia, Didelphidae, *Chacodelphys formosa* (Shamel, 1930): Range extension. *Check List* 3:333–335.
- TETA, P., U. F. J. PARDIÑAS, AND G. D'ELÍA. 2006. Rediscovery of *Chacodelphys*: a South American marsupial genus previously known from a single specimen. *Mammalian Biology* 71:309–314.
- VOSS, R. S., A. L. GARDNER, AND S. A. JANSÁ. 2004. On the Relationships of “*Marmosa*” *formosa* Shamel, 1930 (Marsupialia: Didelphidae), a phylogenetic puzzle from the Chaco of northern Argentina. *American Museum Novitates* 3442:1–18.
- VOSS, R. S., E. E. GUTIÉRREZ, S. SOLARI, R. V. ROSSI, AND S. A. JANSÁ. 2014. Phylogenetic relationships of mouse opossums

- (Didelphidae, *Marmosa*) with a revised subgeneric classification and notes on sympatric diversity. *American Museum Novitates* 3817:1–27.
- VOSS, R. S., AND S. A. JANSÁ. 2003. Phylogenetic studies on didelphid marsupials II. Nonmolecular data and new IRBP sequences: separate and combined analyses of didelphine relationships with denser taxon sampling. *Bulletin of the American Museum of Natural History* 276:1–82.
- VOSS, R. S., AND S. A. JANSÁ. 2009. Phylogenetic relationships and classification of didelphid marsupials, an extant radiation of New World metatherian mammals. *Bulletin of the American Museum of Natural History* 322:1–177.
- VOSS, R. S., B. K. LIM, J. F. DÍAZ-NIETO, AND S. A. JANSÁ. 2013. A new species of *Marmosops* (Marsupialia : Didelphidae) from the Pakaraima highlands of Guyana, with remarks on the origin of the endemic Pantepui mammal fauna. *American Museum Novitates* 3778:1–28.
- VOSS, R. S., D. P. LUNDE, AND S. A. JANSÁ. 2005. On the contents of *Gracilinanus* Gardner and Creighton, 1989, with the description of a previously unrecognized clade of small didelphid marsupials. *American Museum Novitates* 3482:1–34.

Submitted 07 August 2015. Accepted 22 November 2015.

Associate Editor was Jacob A. Esselstyn.